

MAGNET STRENGTH FLUCTUATIONS IN THE SSC LATTICE
PART 2: Frequency Modulation

G.P.Goderre
Texas Accelerator Center
June 1987

Introduction

This is a continuation of SSC-N-305. SSC-N-305 examined the effects of field strength modulation, when the modulation frequency (f_{mod}) was equal to zero (*i.e.*, current offset). The objective of this study is to examine the effect of field strength modulation with modulation frequencies other than zero. To this end, the tracking routine TEAPOT is modified to simulate frequency modulation of the current output from the 10 main SSC magnet power supplies. The amplitude (A_i) and phase (ϕ_i) of the modulation for the i^{th} power supply are chosen randomly. Effects of bore tube shielding¹ are included only when studying 60 Hz modulation frequency. Bore tube shielding is due to the copper coating on the bore tube walls. This coating modifies the amplitude and phase of the modulation inside the bore tube. Figure 1a shows that the bore tube is more effective at shielding the dipole field and it becomes most effective as the modulation frequency increases. Modulation of the field strength is given by the expression:

$$\frac{\Delta B}{B} = R(f_{mod}) \cdot A_i \cdot \sin(2\pi f_{mod} + \phi_i - \phi_R(f_{mod}))$$

where $R(f_{mod})$ and $\phi_R(f_{mod})$ are the amplitude reduction factor and the phase shift produced by the bore tube, respectively. For the particular thickness of copper coating and bore tube radius used in this study, the quantities $R(f_{mod})$ and $\phi_R(f_{mod})$ are shown graphically in figure 1a and 1b, respectively. The amplitudes A_i are chosen randomly using a flat distribution between 0 and 10^{-4} , and the phases ϕ_i are chosen randomly using a flat distribution between 0 and 2π . This study deals with only one set of A_i and ϕ_i ($i = 1, 10$). The particular set used is shown in table 1.

Lattice Settings

As in the previous note (SSC-N-305), the SSC realistic lattice, with clustered-IR's is used. This lattice has a 60° phase advance per cell and is set up using collision optics. Random errors are assigned to each dipole using a gaussian random number generator. The rms width of the gaussian distribution for each of the multipole errors is given in Table 2. The linear tune is adjusted using the correction quadrupoles in the primary arc spool pieces (one focusing and one defocusing quadrupole per cell). The main quadrupole strengths are fixed by the main power supply to which they are connected, and they are modulated along with the main dipoles. For all of the results presented here the x-tune

is set at 78.265 and the y-tune at 78.285. Chromaticity is adjusted using two families of sextupoles located in the primary arc spool pieces. The x and y chromaticity is set to zero. Horizontal and vertical motion is not decoupled in this analysis. However, a modified version of TEAPOT is used which evaluates the 4×4 linear transfer matrix. Therefore the effects of linear coupling can be calculated. Since there are no skew quadrupoles in the system and no solenoids in the IR's, the coupling comes only from higher order multipole feeddown.

Smear

The effect of field strength modulation on the smear is examined. In this study the smear is evaluated at one point in the lattice. It is assumed that if the observation point is moved the smear is not changed. In order for this assumption to be valid, the closed orbit (x_c, x'_c, y_c, y'_c) at the observation point must be known and its effect on the smear must be removed. When the field strength of the magnets is modulated, the closed orbit at the observation point is not a constant. The closed orbit is then a function of turn number as is shown in figure 2a through 2d. Figures 2e through 2h show that the closed orbit in the vertical plane is not affected by the modulation. To simplify the calculations the modulation frequency (f_{mod}) is chosen to be an n^{th} of the revolution frequency (f_{rev}).

$$n \cdot f_{mod} = f_{rev}$$

For the lattice and particle energy being considered here, the revolution frequency is 3614.5 Hz. The modulation frequencies is chosen so that n is equal to 5 and 60 (i.e., 722.9 Hz and 60.24 Hz). In these cases, the modulation repeats itself every n turns. The closed orbit correction to x, x', y, y' is a constant, if the analysis is restricted to observing every n^{th} turn while ignoring the intervening $n - 1$ turns. The smear that is calculated using every n^{th} turn is valid only if the smear is independent of turn number chosen to start the sequence. This point will be clarified at the end of this section. A modified version of TEAPOT² is used to calculate the n -turn closed orbit and the n -turn 4×4 linear transfer matrix T . The n -turn 4×4 linear transfer matrix, when operating on a state vector (x, x', y, y') , transforms it into the state vector after n -turns. The matrix T allows the x-y coupling, the eigentunes, and the smear in the eigendirection to be calculated. The x-y coupling is evaluated using the method discussed in reference 3. The transfer matrix is used to calculate how much the x, x', y, y' directions are tilted relative to the eigendirection (designated as ϕ in ref. 3) for 722.9 Hz and 60.24 Hz modulation. For a particular seed (1234567), the tilt increases with decreasing modulation frequency from ≈ 7 mrad at 722.9 Hz to ≈ 80 mrad at 60.24 Hz. The smear (S_z) is defined as follows:

$$S_z = 2 \cdot \frac{A_z^{max} - A_z^{min}}{A_z^{max} + A_z^{min}}$$

where

$$W_z = A_z^2 / \beta_z$$

$$A_z = \sqrt{z^2 + (\alpha_z z + \beta_z z')^2}$$

$$z = x - x_c ; y - y_c$$

$$z' = x' - x'_c ; y' - y'_c$$

The expression for W_z , when linear coupling is present, is given in reference 3, and it is used to calculate the smear in the eigendirections (u, v).

Figures 3a and 3b show the smear *vs* launch amplitude, without field strength modulation, in the horizontal and vertical plane, respectively. Here the launch amplitude is a particular value ($x' = y' = 0$) of x, x' , and y, y' , which lie on the invariant ellipses W_x , and W_y , respectively. It is generally assumed that the smear is independent of the particular initial point as long as it lies on the invariant ellipse. There are four curves in each figure. Each curve represents a different distribution of random errors in the dipole magnets. Figure 4a,b and 5a,b show how the smear varies with launch amplitude, when the field strength is modulated by 722.9 Hz and 60.24 Hz, respectively. Comparison of these figures indicates that modulation has little effect on the smear, when the launch amplitude is less than $W_x = W_y < 0.15 \times 10^{-6}$ meters (or $A_x = A_y < 7.0$ mm at $\beta_{x,y} = 320$ meters). This statement is quantified by defining the linear aperture as that launch amplitude (A_x or A_y evaluated at $\beta = 320$ meters) for which the smear first reaches 30%, in either the x, x' or y, y' plane. Table 3 shows the linear aperture for each of the cases discussed above. Averaging these results for the different random seeds, shows that the linear aperture gets slightly smaller as the modulation frequency is increased. In the worst case with 722.9 Hz, the linear aperture is 6.4 ± 0.5 mm, in comparison to 7.4 ± 0.5 mm without modulation. However, bore tube shielding is ignored in the case of 722.9 Hz modulation. Figure 1 gives $R(722.9\text{Hz}) \approx 0.10$. Hence, if bore tube shielding is included, the effect on the linear aperture would be greatly reduced. In the case of 60.24 Hz, where bore tube shielding is included, the average linear aperture is 6.7 ± 0.7 mm. For launch amplitudes greater than $W_x = W_y \approx 0.15 \times 10^{-6}$ meters, the smear in the horizontal direction is noticeably increased by the modulation. Whereas, in the vertical direction the smear with and without modulation are comparable. The large amplitude behavior is quantified by defining a dynamic aperture. The dynamic aperture is the largest launch amplitude for which the particle remains in the beam pipe for at least 500 turns. Table 3 shows the dynamic aperture for each of the cases discussed above. The dynamic aperture in all cases are comparable. There is only one case where the 722.9 Hz modulation shows a large reduction in the dynamic aperture, but here again bore tube shielding should help in this case.

Figure 6a,b show the smear *vs* launch amplitude, for 60 Hz modulation, in the u, v eigendirections, respectively. Comparison of figures 6a,b with 5a,b show that the x-y coupling increases the smear for launch amplitudes less than $W_x = W_y < 0.15 \times 10^{-6}$ meters. At this point, it is worth examining the assumption that the smear is independent of the turn number. Figure 7a,b shows the u, x smear *vs* turn number for 60.24 Hz modulation, with a particular random error seed (1234567). The smear is a function of which turn number is chosen as the observation point or turn. As before, starting from the observation turn, every n^{th} turn is observed thereafter. The closed orbit and 4×4 linear n -turn transfer matrix is calculated for the new observation point. However, the particle is still

launched at turn zero with $W_x = W_y$. Therefore, the initial amplitude at the observation point is not in general the launch amplitude. These results indicate that the turn by turn smear is in general greater than the smear calculated using a particular initial turn then every n^{th} turn thereafter. Figure 7a,b give an estimate of the increase to expect. Therefore, the linear aperture is somewhat smaller than what is shown in table 3. The 4×4 linear n -turn transfer matrix is used to calculate the change in x-y coupling from turn to turn, which is $\approx 80 \pm 10$ mrad, for the particular random error seed tested (1234567). It is not clear what would happen if we tried to remove the coupling with the skewed quadrupoles in the spool pieces. It seems apparent that it can not be totally removed since there is a variation in the amount of x-y coupling from turn to turn.

Tune

The tune for a given launch amplitude is calculated using the tracking results from TEAPOT. The x and y positions of the particle after every n turns are fourier analyzed. The maximum fourier component (for each launch amplitude) is taken to be the tune for that particular amplitude. The tune defined in this manner differs from the normal single turn tune by a factor of n . Therefore, the normal single turn tune shift $\Delta\nu$ is equal to a n -turn tune shift of $n \cdot \Delta\nu$. Figures 8a and 8b show the variation of tune with launch amplitude without field strength modulation. Figures 9a,b and 10a,b show the tune *vs* launch amplitude when the field strength modulation is 722.9 Hz and 60.24 Hz, respectively. comparison of the tunes with and without modulation confirms the conclusion of SSC-N-305, which states that the tune variation should not be affected by field strength modulation. It should be noted that for $f_{mod} = 60.24$ Hz the tune spectrum was not a sharp peak when the launch amplitude ($W_x = W_y$) was greater than 0.10×10^{-6} meters. In a typical tune spectrum, without modulation, the peak would be about 4 db above background. However, for 60.24 Hz modulation this was reduce to 2db at a launch amplitude ($W_x = W_y$) of 0.20×10^{-6} meters. Also, the peak was broader for 60.24 Hz modulation. Since this anomalous behavior only occur at very large amplitudes it should not create a problem.

One interesting result occurred when examining a particular random seed (7654321) with 60.24 Hz modulation. When the x and y tunes were 78.265 and 78.285, it is found from the 4×4 linear n -turn transfer matrix that the eigentunes do not lie on the unit circle. The eigentunes in complex space look similar to Fig. 2d in Courant and Snyder page 31 (ANNALS OF PHYSICS: 3, 1-48 (1958)). Courant and Snyder state, "that this behavior cannot arise without coupling, and represents a type of instability that is generated only by the coupling." However, when the x tune is changed by ± 0.0002 the instability disappeared. No long-term tracking was done to examine what would happen to a particle due to this instability. For this particular random seed, the linear horizontal tune is set to 78.2652, in this analysis (figures 5a and 10a) instead of 78.265.

Conclusions

There is no evidence that field strength modulation ($\frac{\Delta B}{B}$) at the 10^{-4} level causes any real reduction in either the linear or dynamic aperture. Nor does changing the distribution of random errors in the dipole magnets (*i.e.*, random seed). It should be noted that this conclusion is based on a single set of A_i and ϕ_i ($i = 1, 10$). The fact that the smear (for slow modulation frequencies) is a function of turn number could effect this conclusion and may need to be examined more closely. However, this effect may be an artifact of how the launch amplitude is defined.

Field strength modulation produces x-y coupling. The amount of coupling depends on the modulation frequency. The slower the modulation frequency the stronger the coupling. In the case of 60.24 Hz modulation the strength of the coupling is different for each turn, repeating every 60 turns. This may contribute to the variation of the smear with turn number.

The closed orbit deviation due to field strength modulation is a simple sine wave:

$$z_c \sin\left(\frac{2\pi}{n} n_t + \chi\right)$$

where z_c is either x_c or x'_c , n_t is the turn number and χ is an arbitrary phase angle. This simple behavior is somewhat unexpected since A_i and ϕ_i are randomly chosen. It may be interesting to examine the closed orbit for different sets of A_i 's and ϕ_i 's. Figure 2a through 2d indicate the maximum deviation in the closed orbit x_c is independent of modulation frequency, whereas the maximum deviation in the closed orbit x'_c is larger for slower frequencies.

The tune variation with launch amplitude, within the linear aperture, is not affected by the field strength modulation for any of the cases studied here.

Sector	Power Supply i	Phase ϕ_i (rad)	Amplitude A_i (10^{-4})
ARC	1	3.453	0.6547
ARC	2	2.781	0.9951
ARC	3	4.620	0.2209
ARC	4	4.086	0.8202
ARC	5	1.578	0.9010
ARC	6	4.716	0.2081
ARC	7	2.589	0.6725
ARC	8	2.364	0.1535
LOW β	9	1.524	0.1159
MEDIUM β	10	2.346	0.5831

Table 1: The particular set of phase angles (ϕ_i) and amplitudes (A_i) given to the i^{th} power supply. The set was chosen using a random number generator which generated random numbers between 0 and 2π for ϕ_i and 0 and 10^{-4} for A_i .

n	a_n 10^{-4} cm^{-n}	b_n 10^{-4} cm^{-n}
0	0.0000	0.000
1	0.0000	0.000
2	0.6100	0.400*
3	0.6900	0.350
4	0.1400	0.590
5	0.1600	0.059
6	0.0340	0.075
7	0.0300	0.016
8	0.0064	0.021
9	0.0056	0.003

Table 2: Random errors are assigned to each dipole using a gaussian random number generator. The sigma associated with the gaussian distribution for each of the multipole errors (a_n, b_n) is shown. The following expression define these errors:

$$(LB_y + iLB_x) = B_0 L + B_0 L \sum (b_n + ia_n)(x + iy)^n$$

Random seed	f_{mod} Hz	Linear Aperture mm	Dynamic Aperture mm
1234567	0.00	7.5	$9.5^{+0.1}_{-0.0}$
	60.24	7.7	$9.6^{+0.1}_{-0.0}$
	722.90	6.1	$7.2^{+0.1}_{-0.0}$
7654321	0.00	7.9	$10.6^{+0.8}_{-0.0}$
	60.24	6.2	$9.8^{+0.8}_{-0.0}$
	722.90	7.0	$9.8^{+0.8}_{-0.0}$
6543217	0.00	6.8	$9.8^{+0.8}_{-0.0}$
	60.24	6.4	$9.8^{+0.8}_{-0.0}$
	722.90	6.1	$8.9^{+0.8}_{-0.0}$
5432176	0.00	7.0	$8.9^{+0.8}_{-0.0}$
	60.24	6.5	$9.8^{+0.8}_{-0.0}$
	722.90	6.2	$8.9^{+0.8}_{-0.0}$
Average	0.00	7.3 ± 0.5	10.0 ± 0.8
	60.24	6.7 ± 0.7	10.0 ± 0.8
	722.90	6.4 ± 0.5	9.0 ± 1.2

Table 3: The linear and dynamic aperture is tabulated for various modulation frequencies and random error distributions (random seeds). The final column shows the average effect of the different different random seeds at the three modulation frequencies studied.

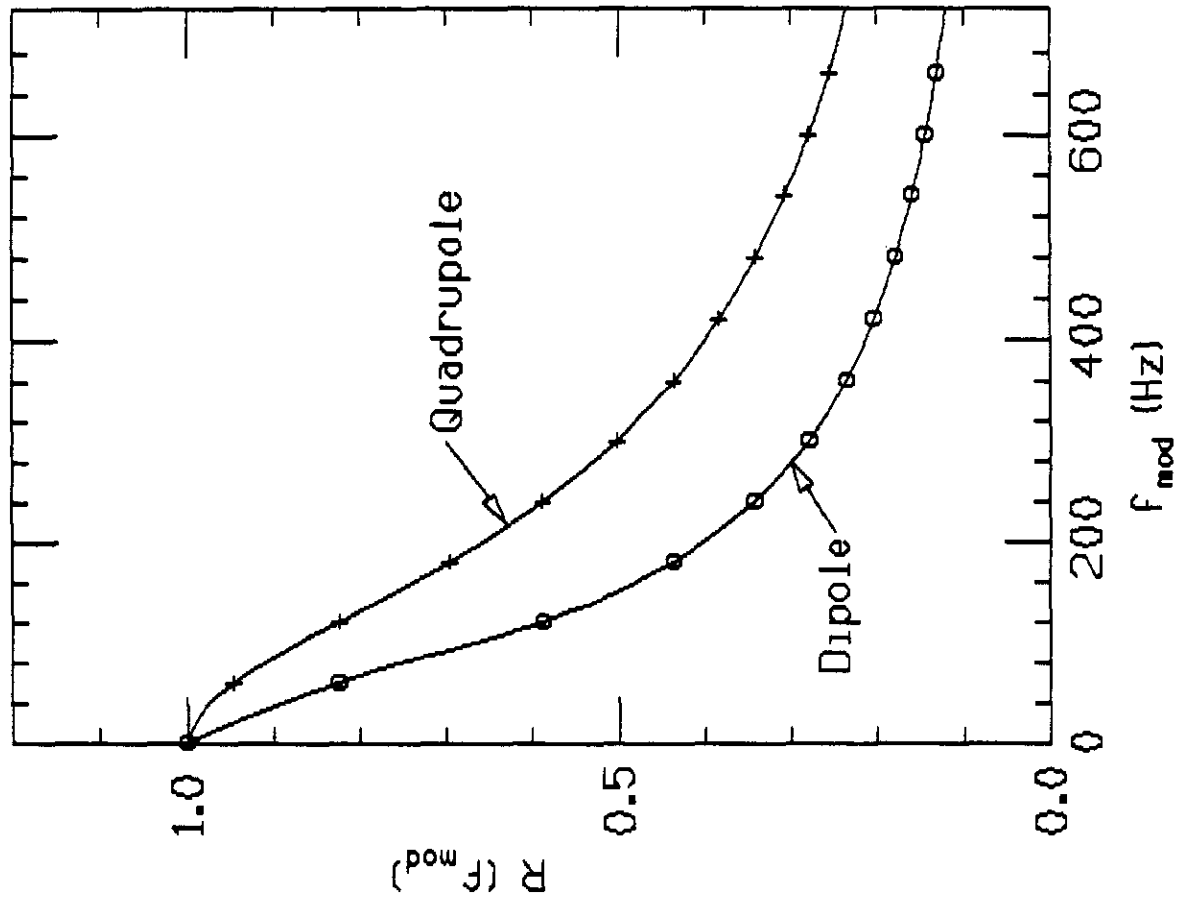


Figure 1a: The amplitude reduction factor vs the modulation frequency, in the SSC dipoles and quadrupoles, produced by bore tube shielding.

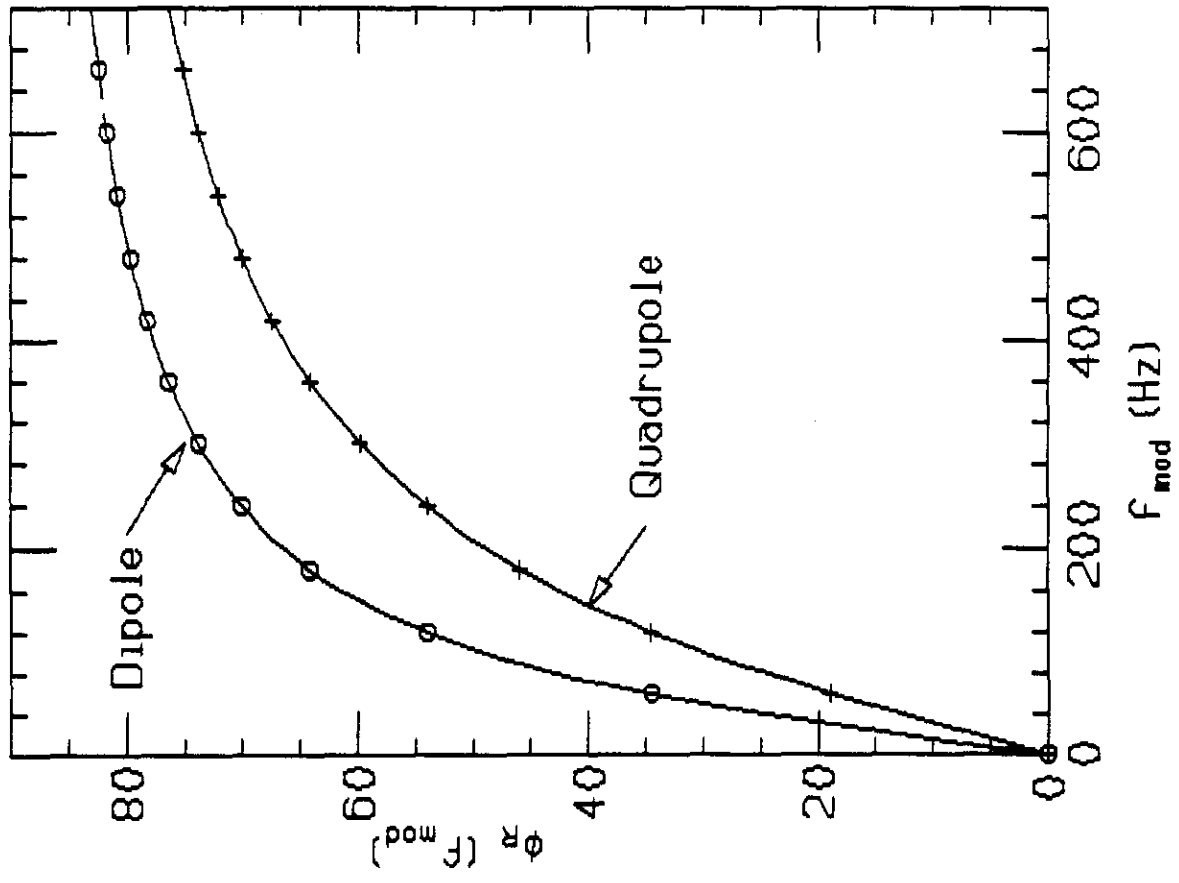


Figure 1b: The phase shift vs the modulation frequency, in the SSC dipoles and quadrupoles, produced by bore tube shielding.

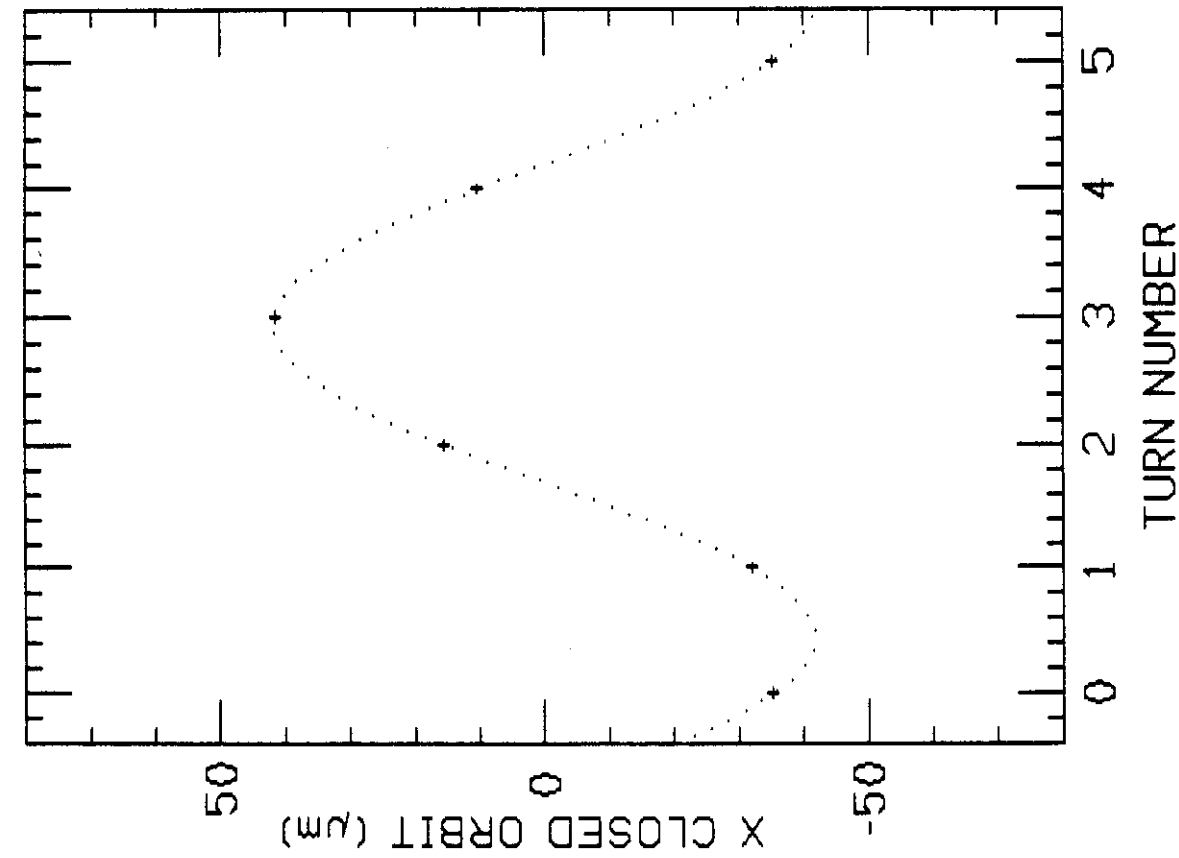


Figure 2a: Closed orbit deviation (x_c) vs turn number with 722.9 Hz field strength modulation. The dotted line is a fit of the 5 data points to a sine function.

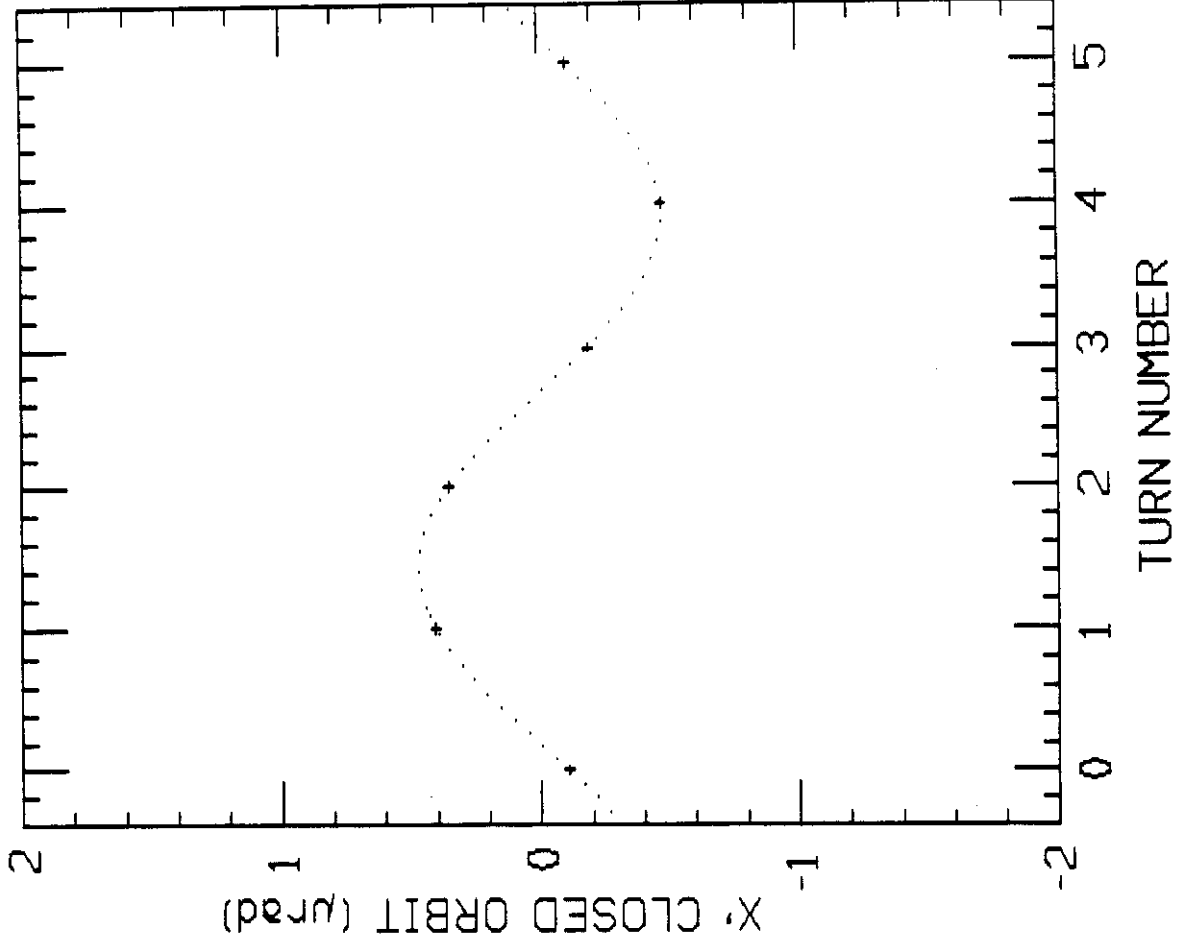


Figure 2b: Closed orbit deviation (x_c') vs turn number with 722.9 Hz field strength modulation. The dotted line is a fit of the 5 data points to a sine function.

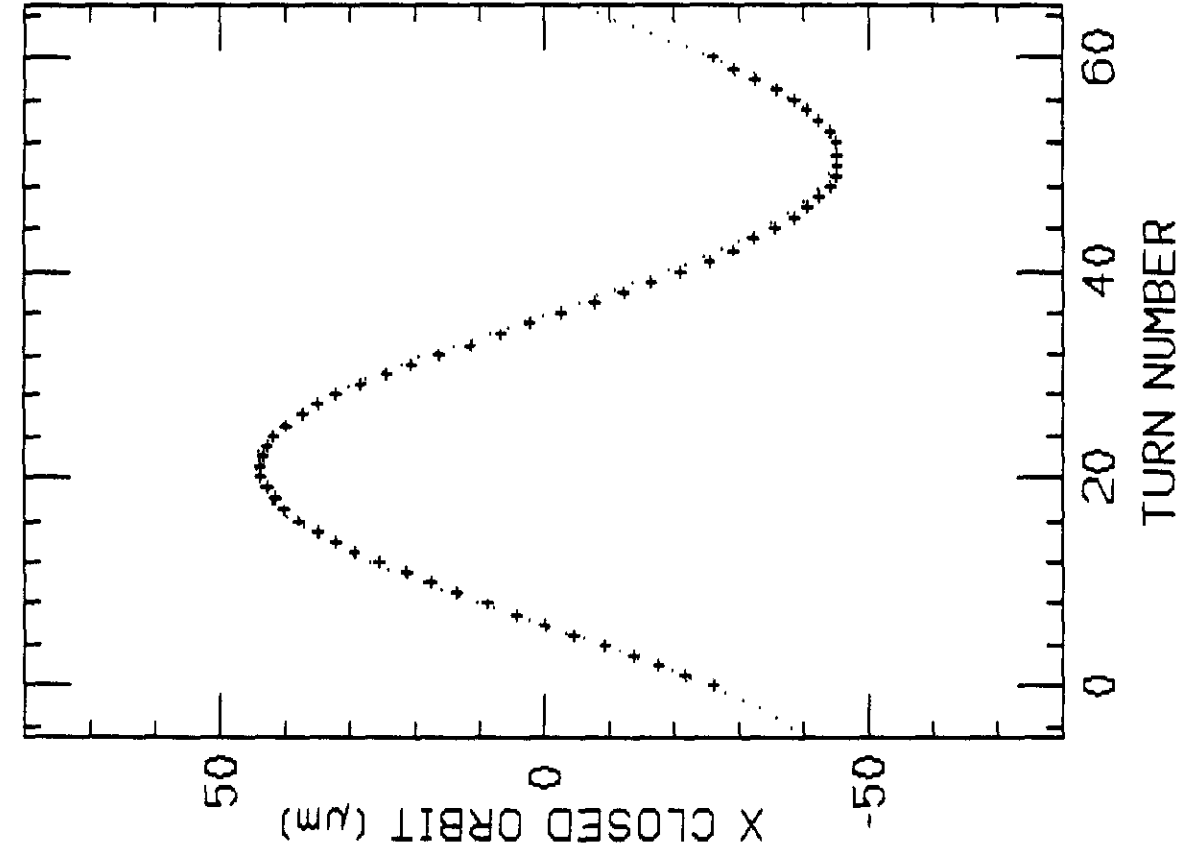


Figure 2c: Closed orbit deviation (x_c) vs turn number with 60.24 Hz field strength modulation. The dotted line is a fit of the 60 data points to a sine function.

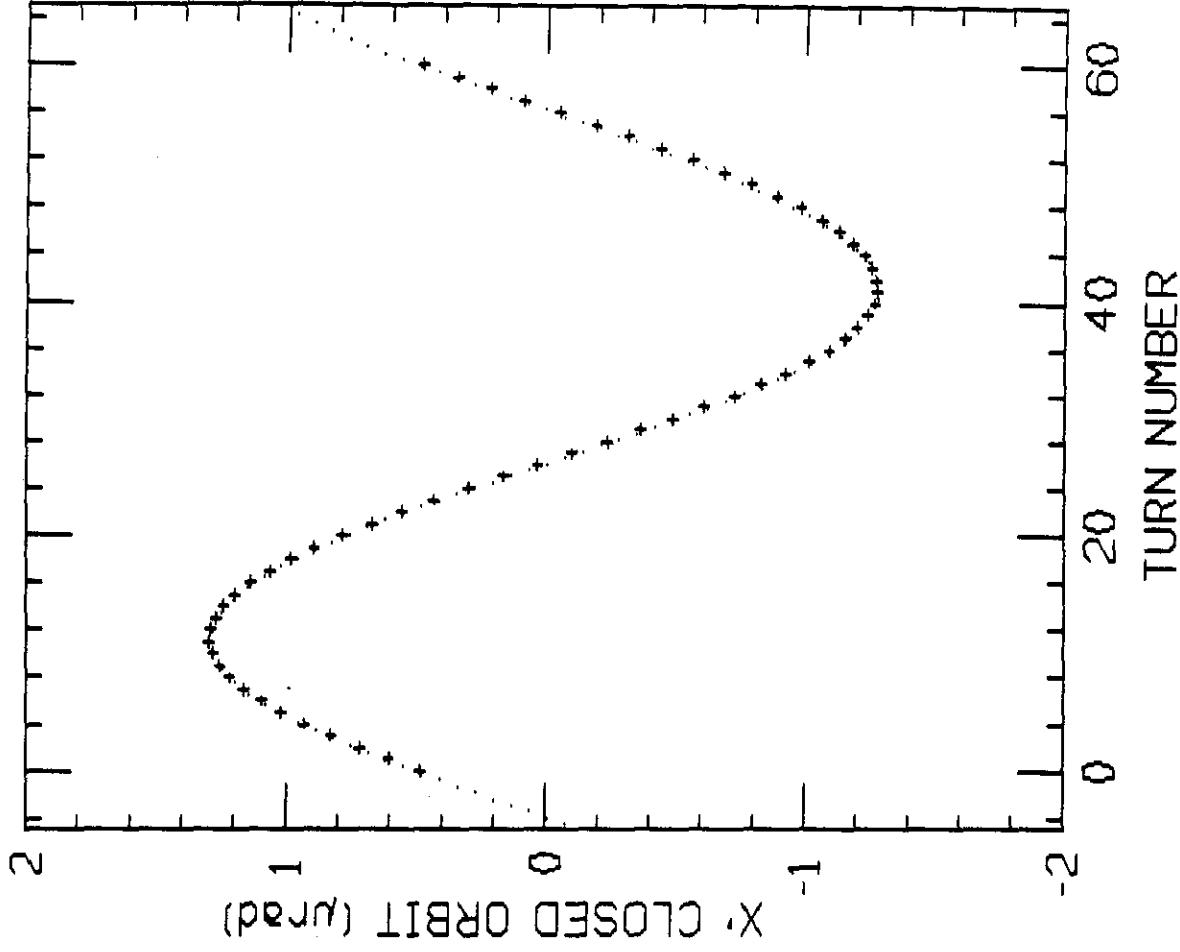


Figure 2d: Closed orbit deviation (x_c) vs turn number with 60.24 Hz field strength modulation. The dotted line is a fit of the 60 data points to a sine function.

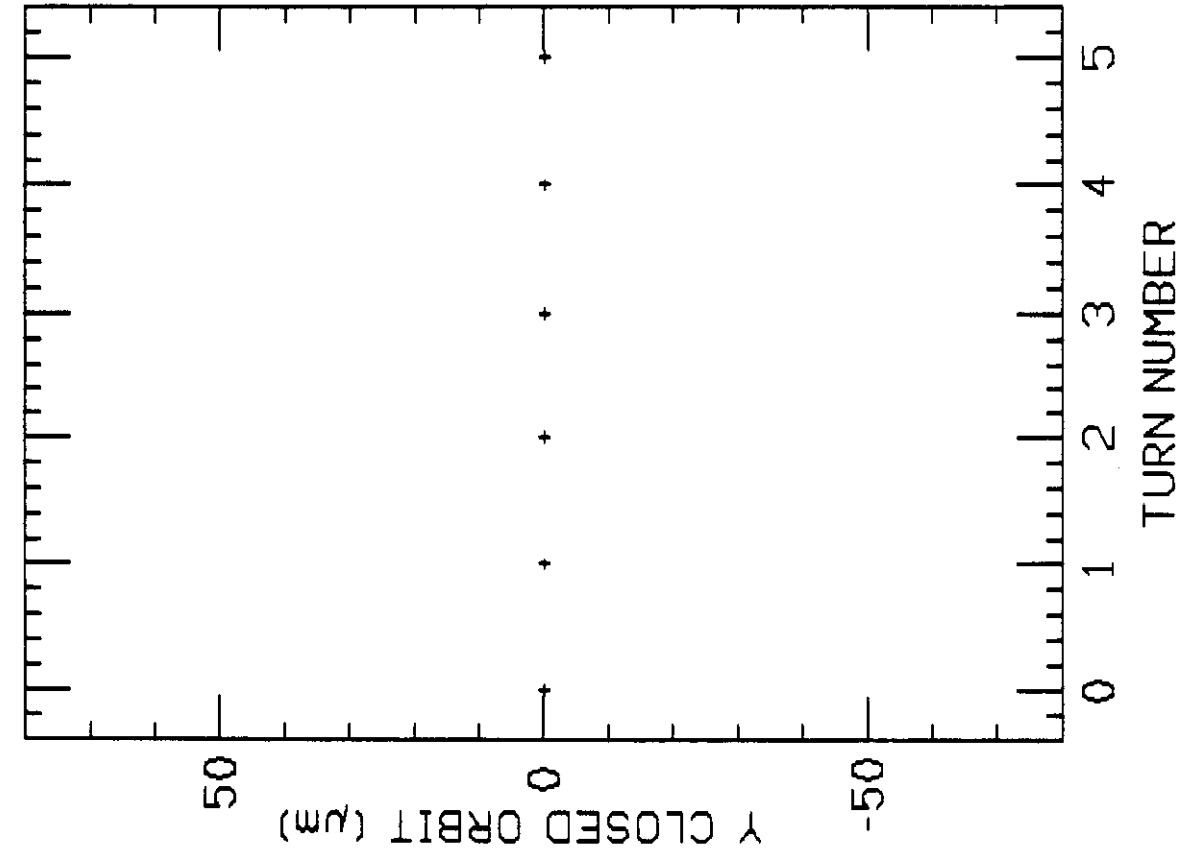


Figure 2e: Closed orbit deviation (y_c) vs turn number with 722.9 Hz field strength modulation. There is no noticeable change in y_c with modulation.

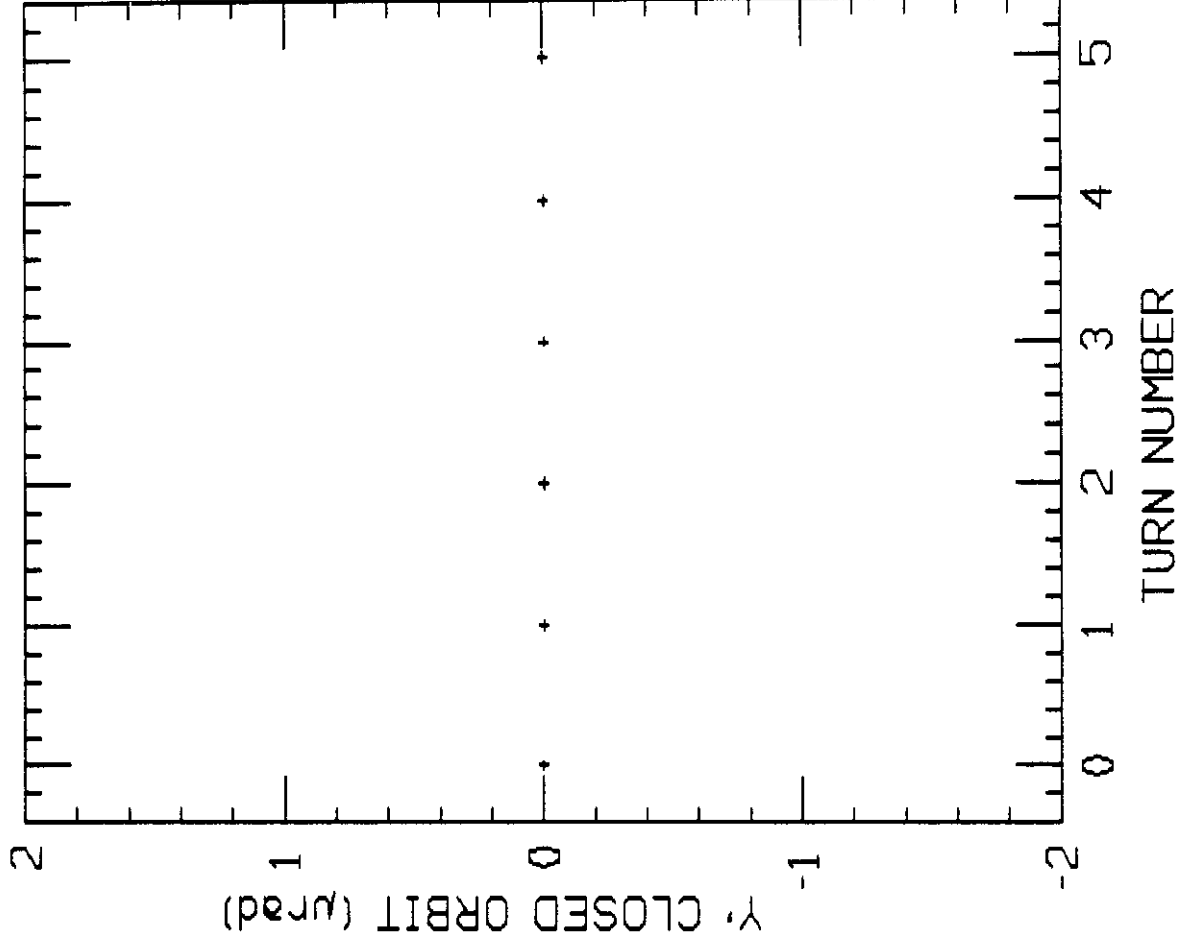


Figure 2h: Closed orbit deviation (y_c') vs turn number with 722.9 Hz field strength modulation. There is no noticeable change in y_c' with modulation.

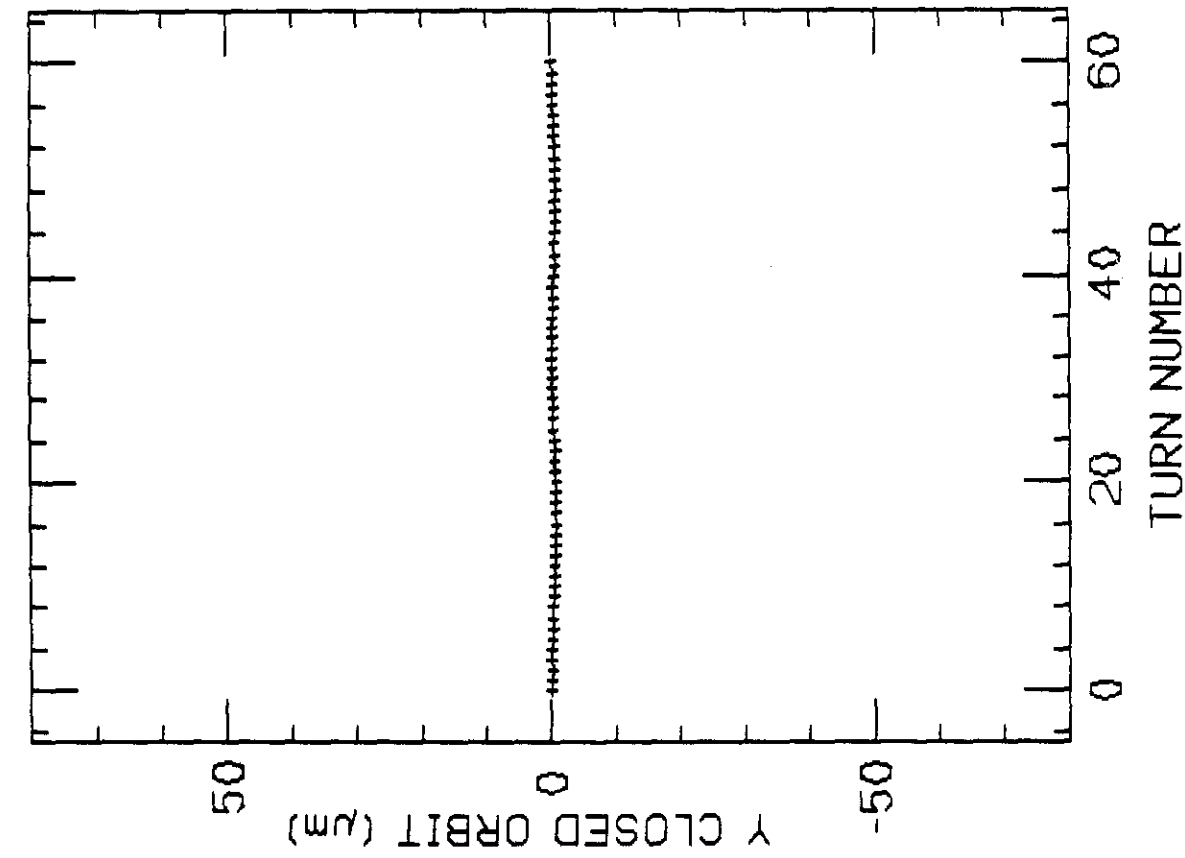


Figure 2q: Closed orbit deviation (y_c) vs turn number with 60.24 Hz field strength modulation. There is no noticeable change in y_c with modulation.

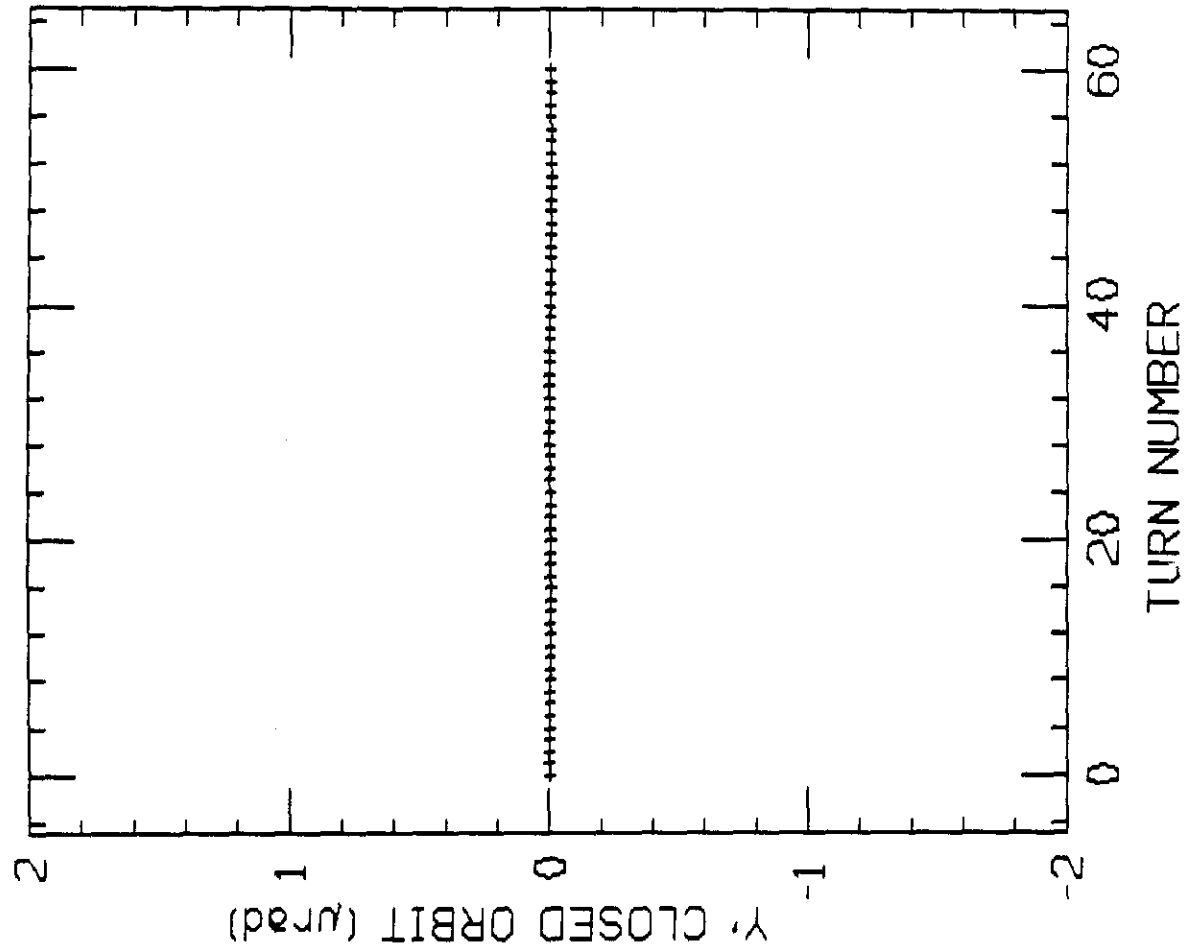


Figure 2h: Closed orbit deviation (y_c) vs turn number with 60.24 Hz field strength modulation. There is no noticeable change in y_c with modulation.

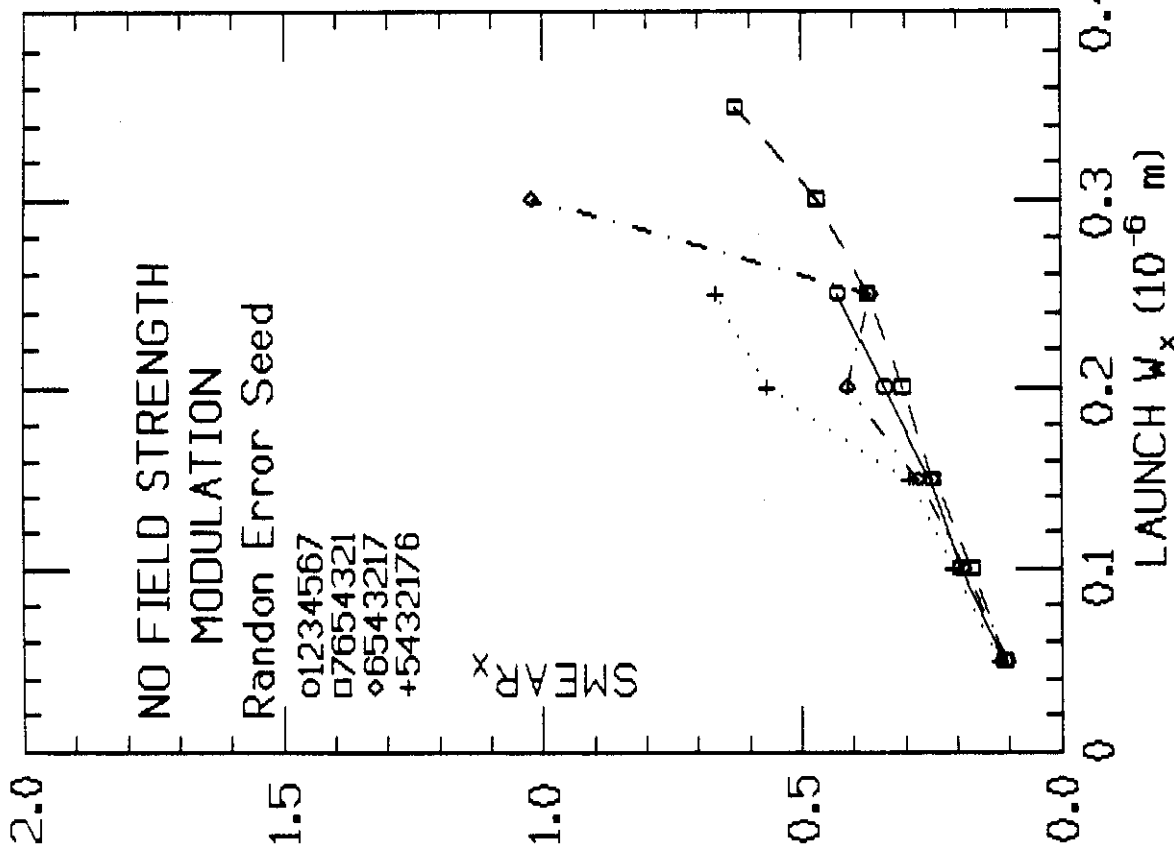


Figure 3a: The smear in the horizontal plane vs launch amplitude without field strength modulation.

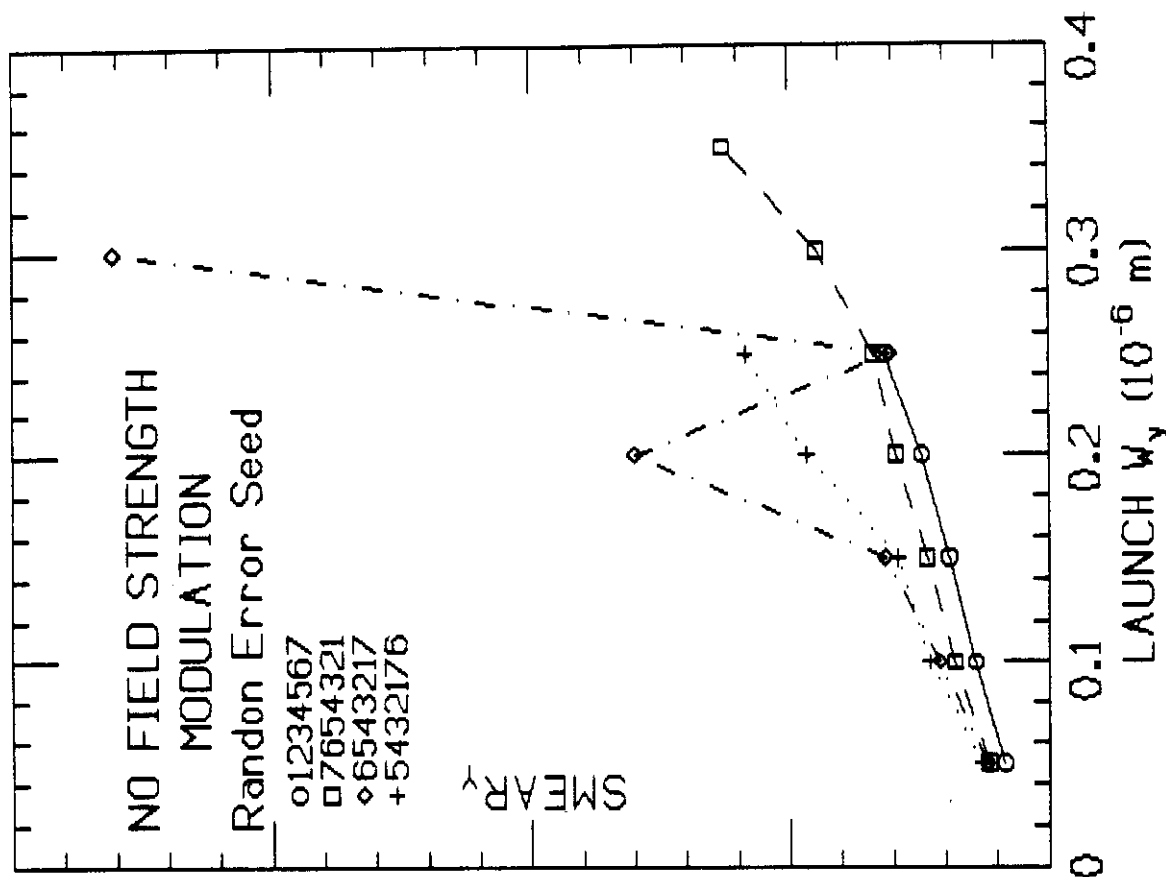


Figure 3b: The smear in the vertical plane vs launch amplitude without field strength modulation.

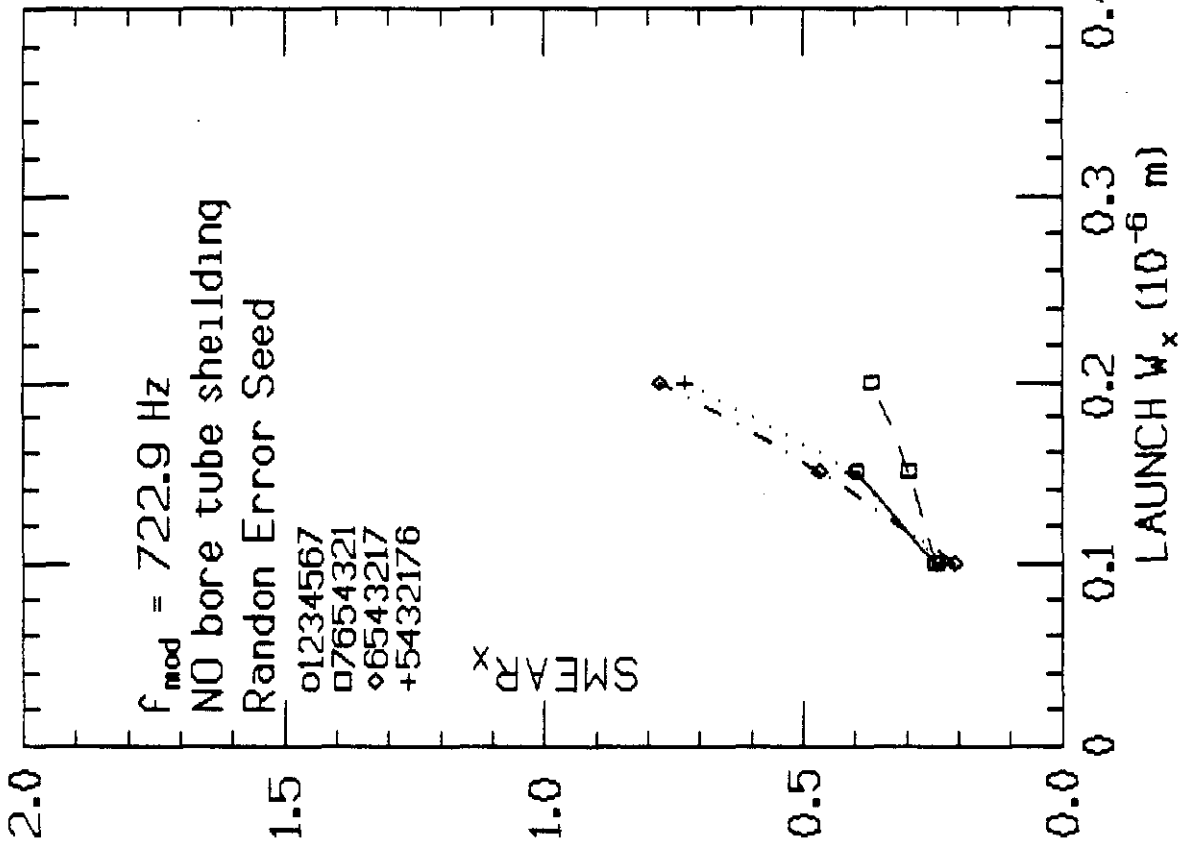


Figure 4a: The smear in the horizontal plane vs launch amplitude with a 722.9 Hz modulation frequency and average $\Delta B/B = 0.5 \times 10^{-4}$.

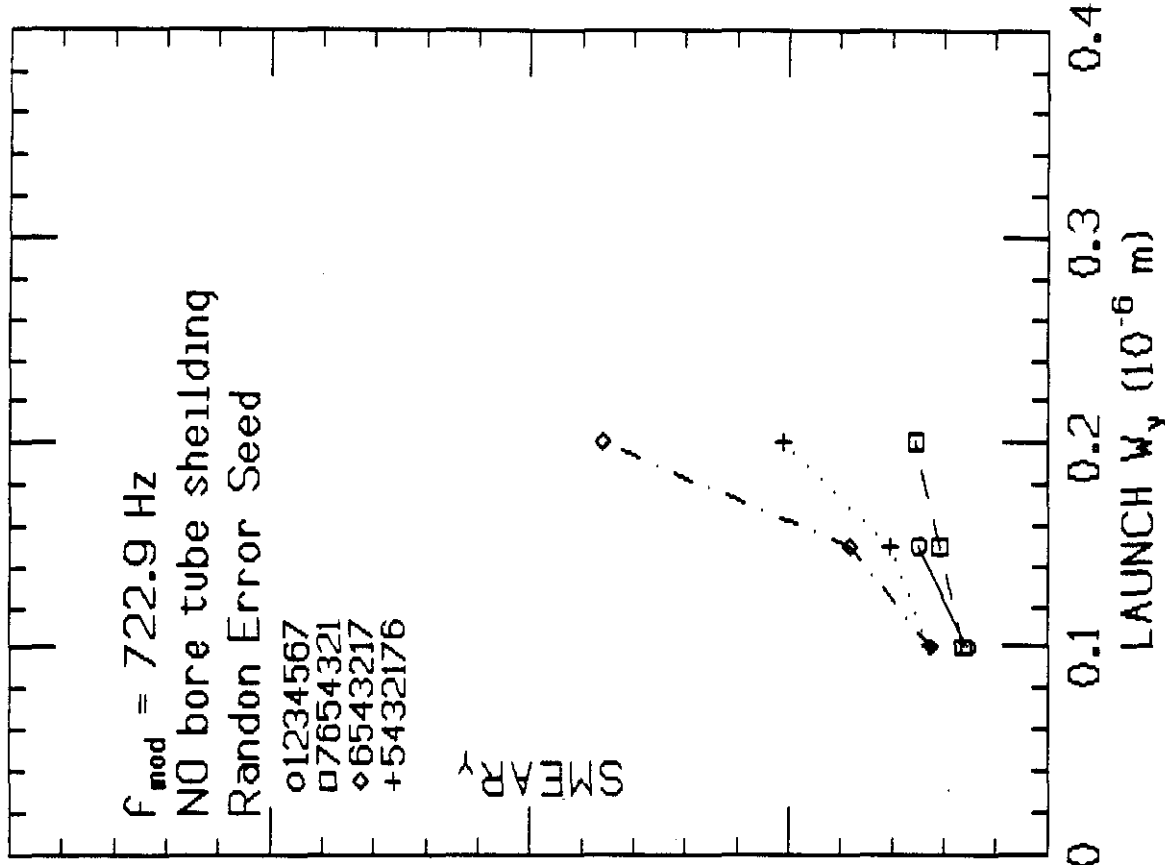


Figure 4b: The smear in the vertical plane vs launch amplitude with a 722.9 Hz modulation frequency and average $\Delta B/B = 0.5 \times 10^{-4}$.

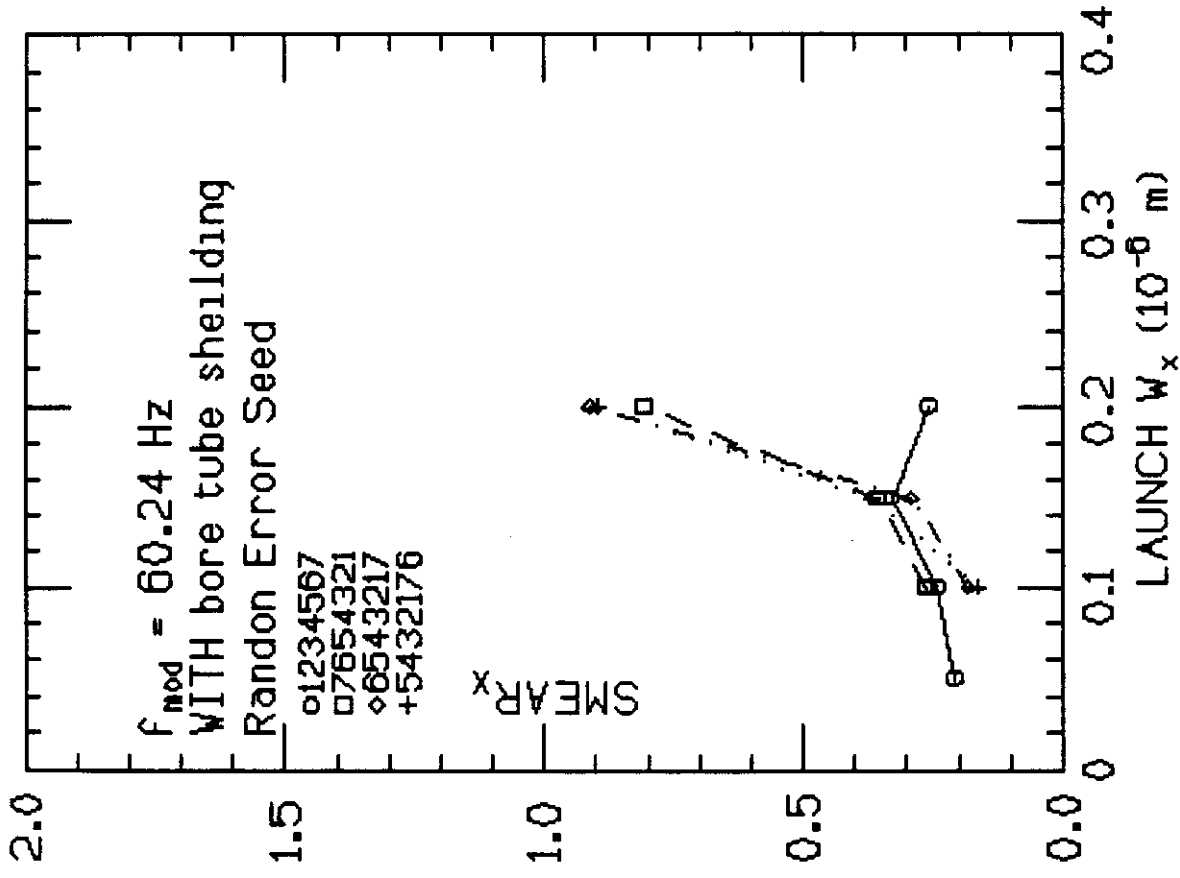


Figure 5a: The smear in the horizontal plane vs launch amplitude with a 60.24 Hz modulation frequency and average $\Delta B/B = 0.5 \times 10^{-4}$.

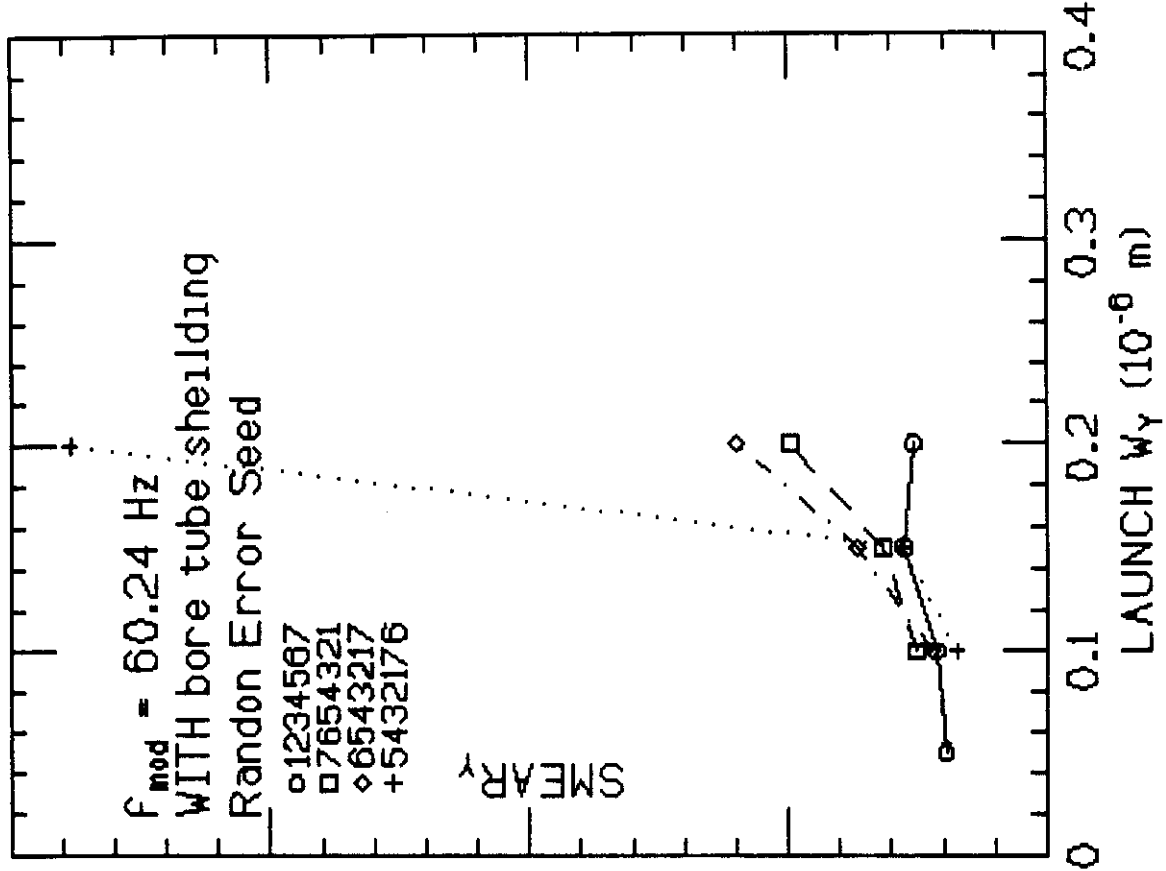


Figure 5b: The smear in the horizontal plane vs launch amplitude with a 60.24 Hz modulation frequency and average $\Delta B/B = 0.5 \times 10^{-4}$.

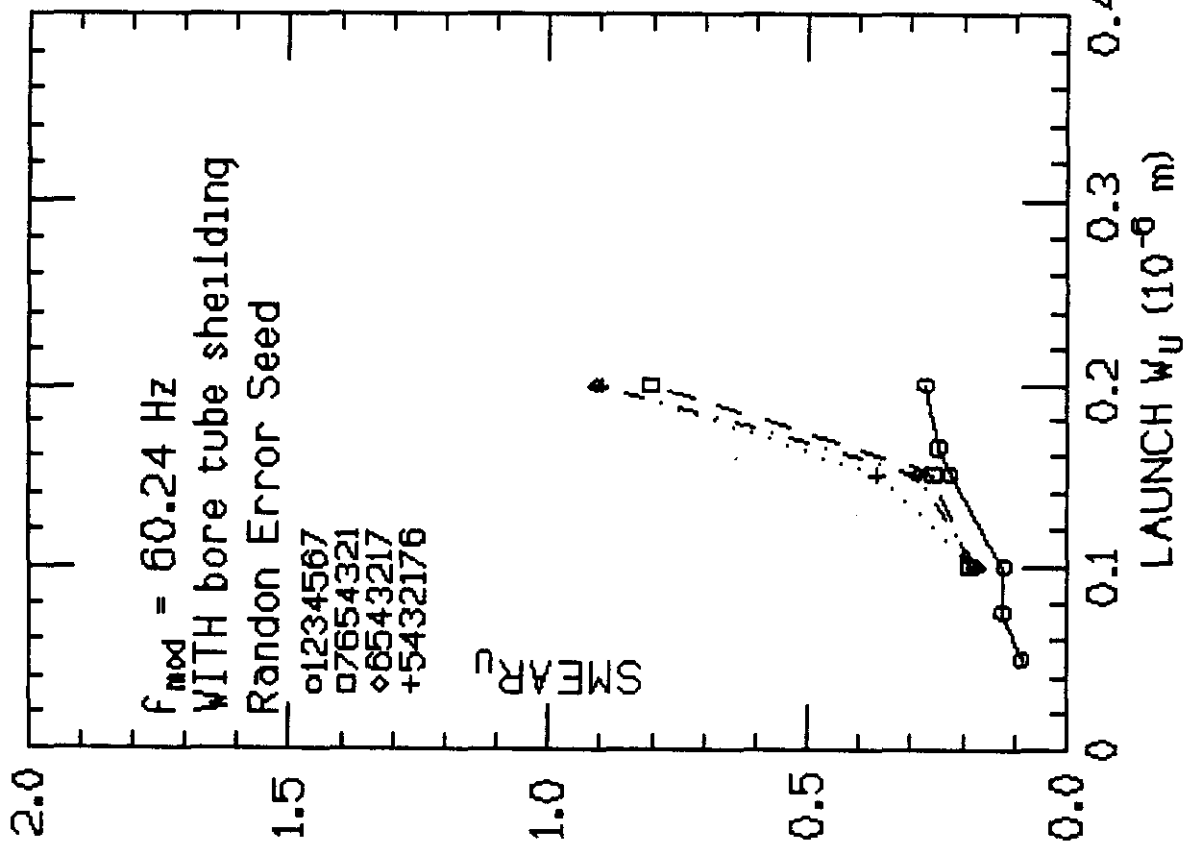


Figure 6a: The smear in the U eigendirection vs launch amplitude with a 60.24 Hz modulation frequency and average $\Delta B/B = 0.5 \times 10^{-4}$.

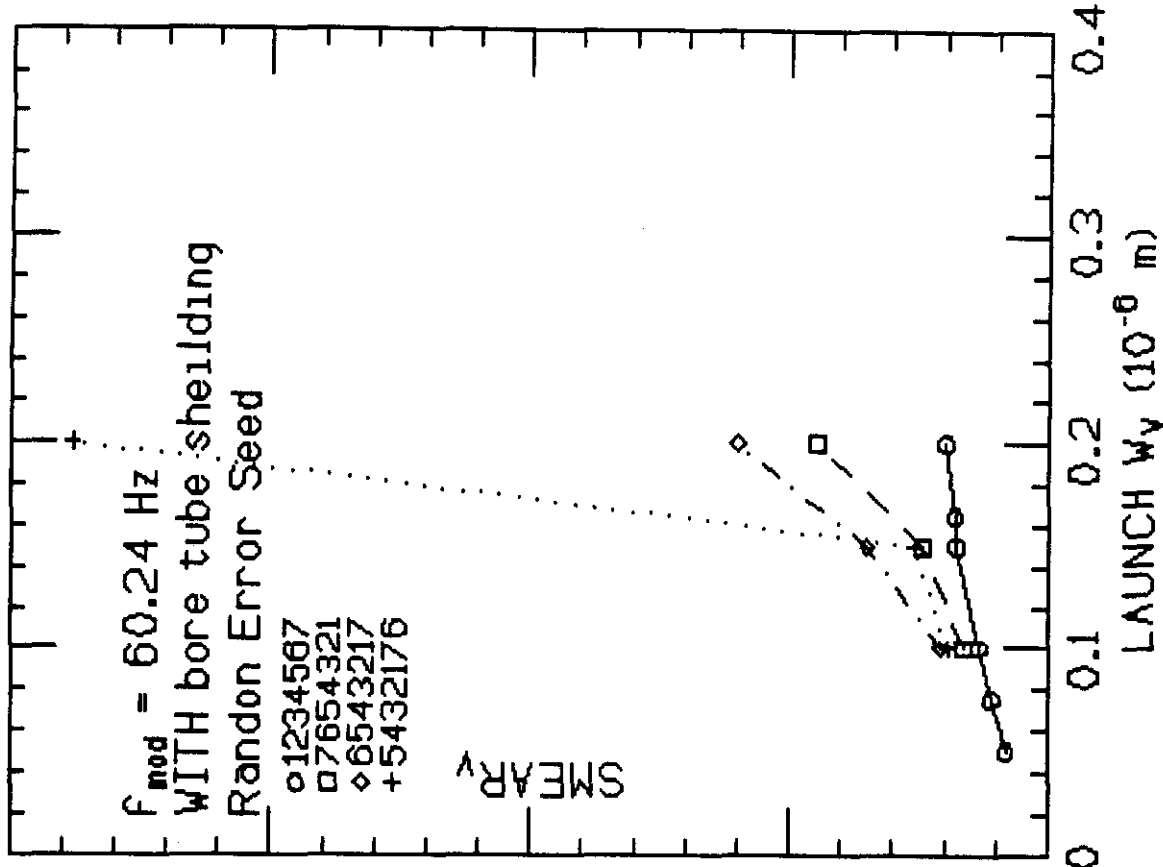


Figure 6b: The smear in the V eigendirection vs launch amplitude with a 60.24 Hz modulation frequency and average $\Delta B/B = 0.5 \times 10^{-4}$.

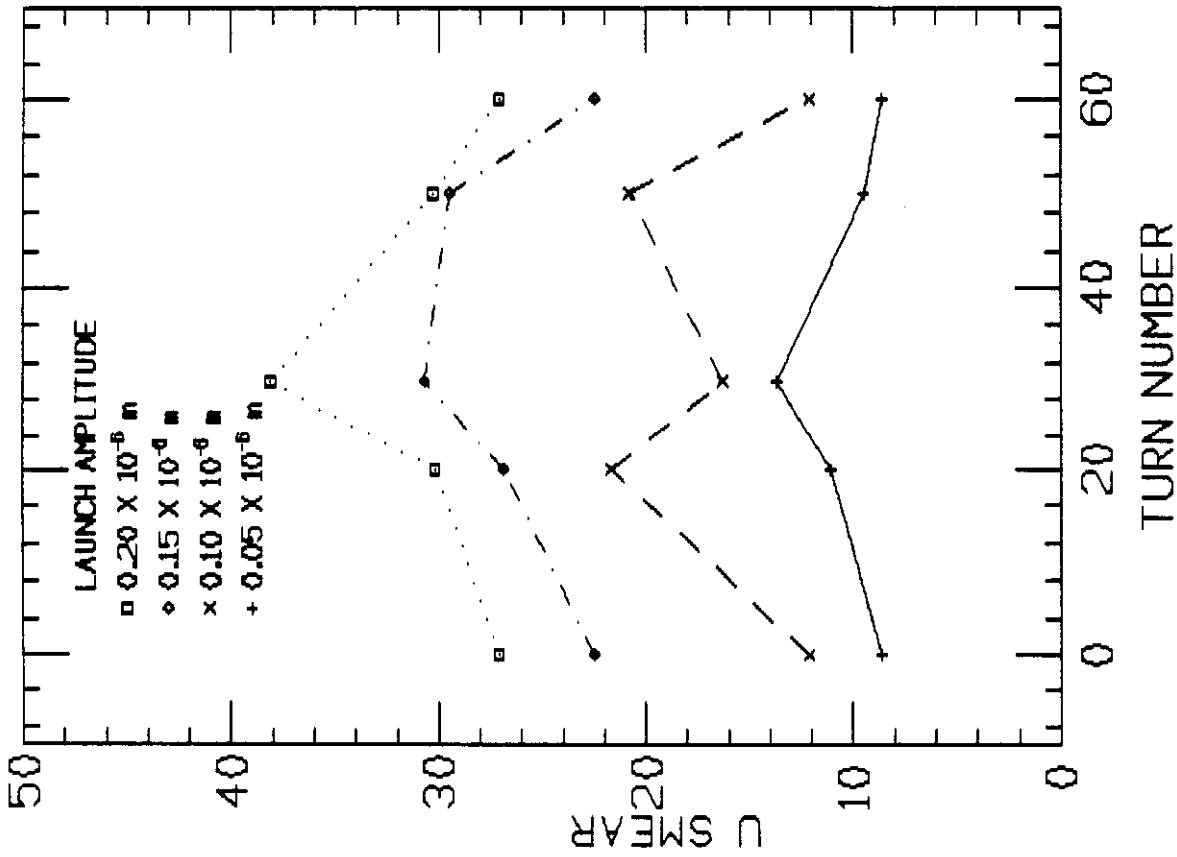


Figure 7a: The smear in the U-eigen-direction vs turn number with 60.24 Hz field strength modulation.

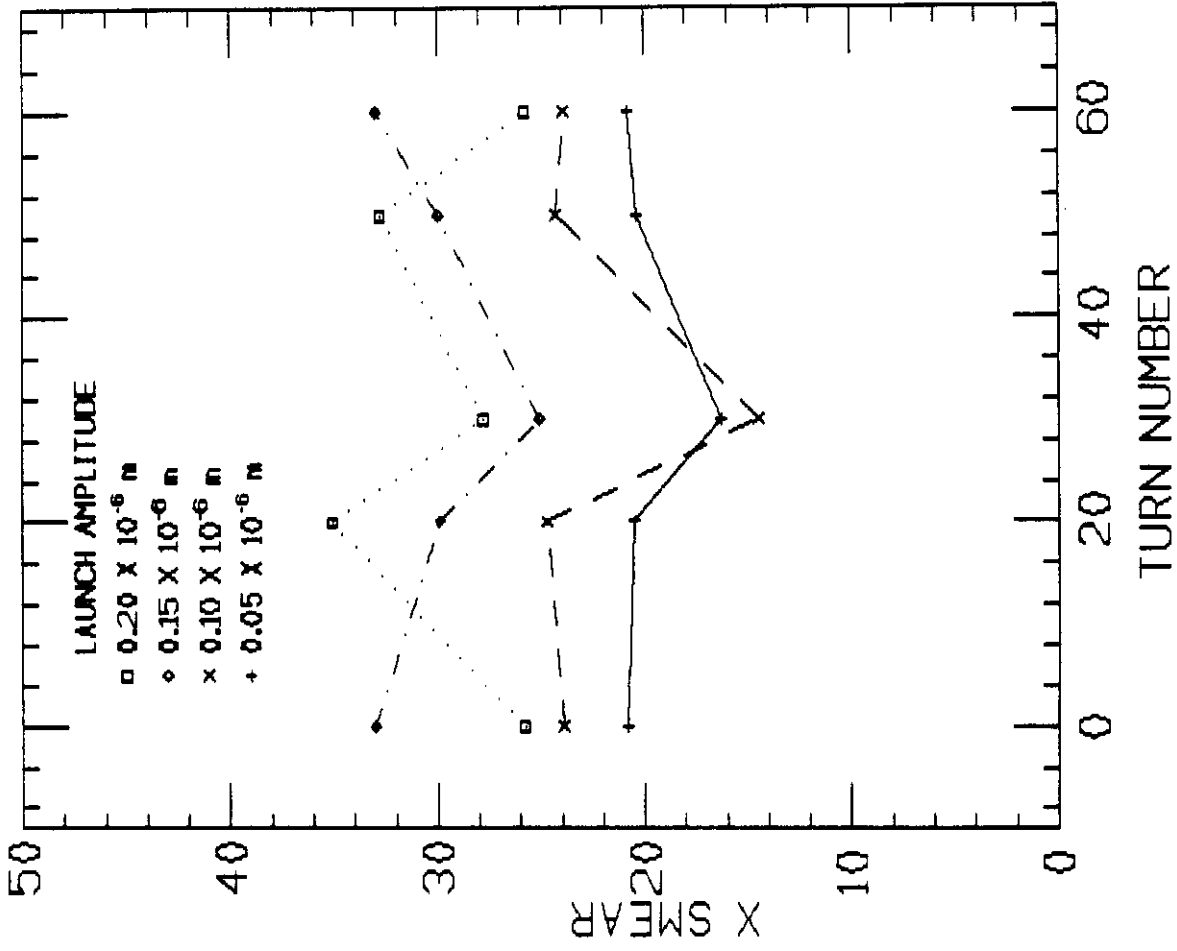


Figure 7b: The smear in the X-direction vs turn number with 60.24 Hz field strength modulation.

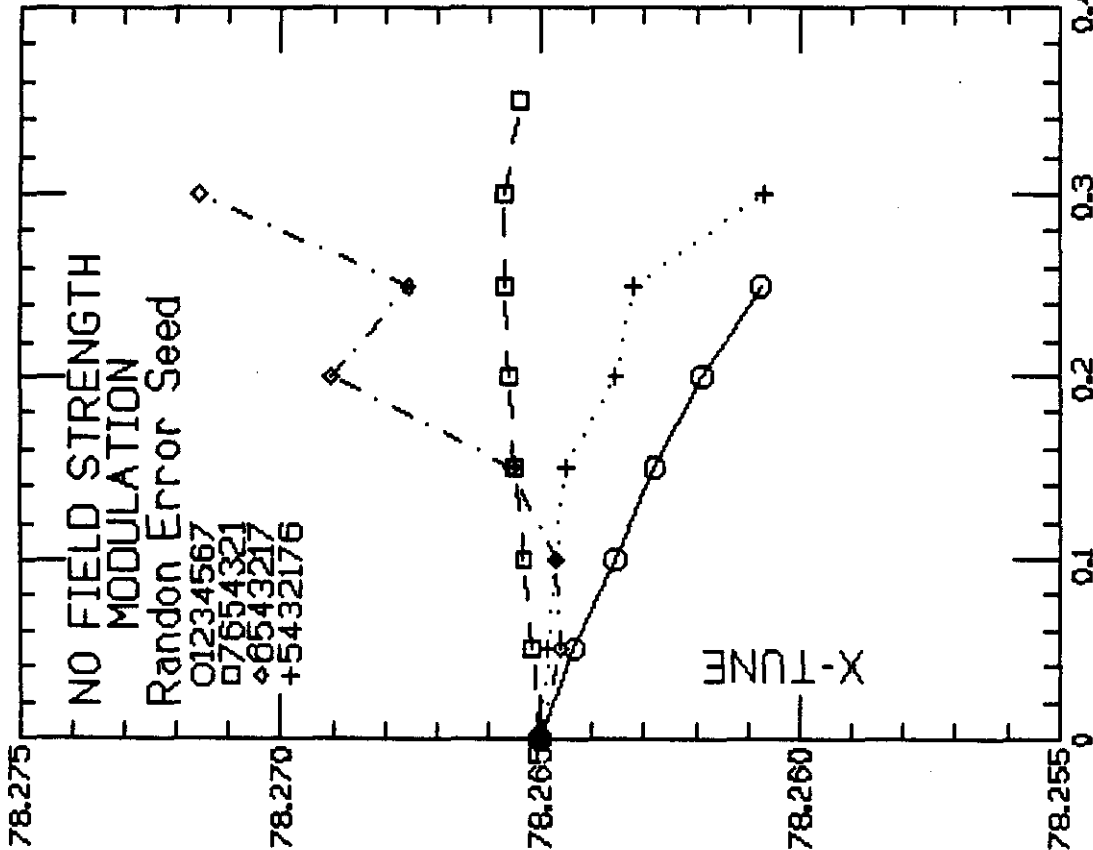


Figure 8a: The tune in the horizontal direction vs launch amplitude without field strength modulation.

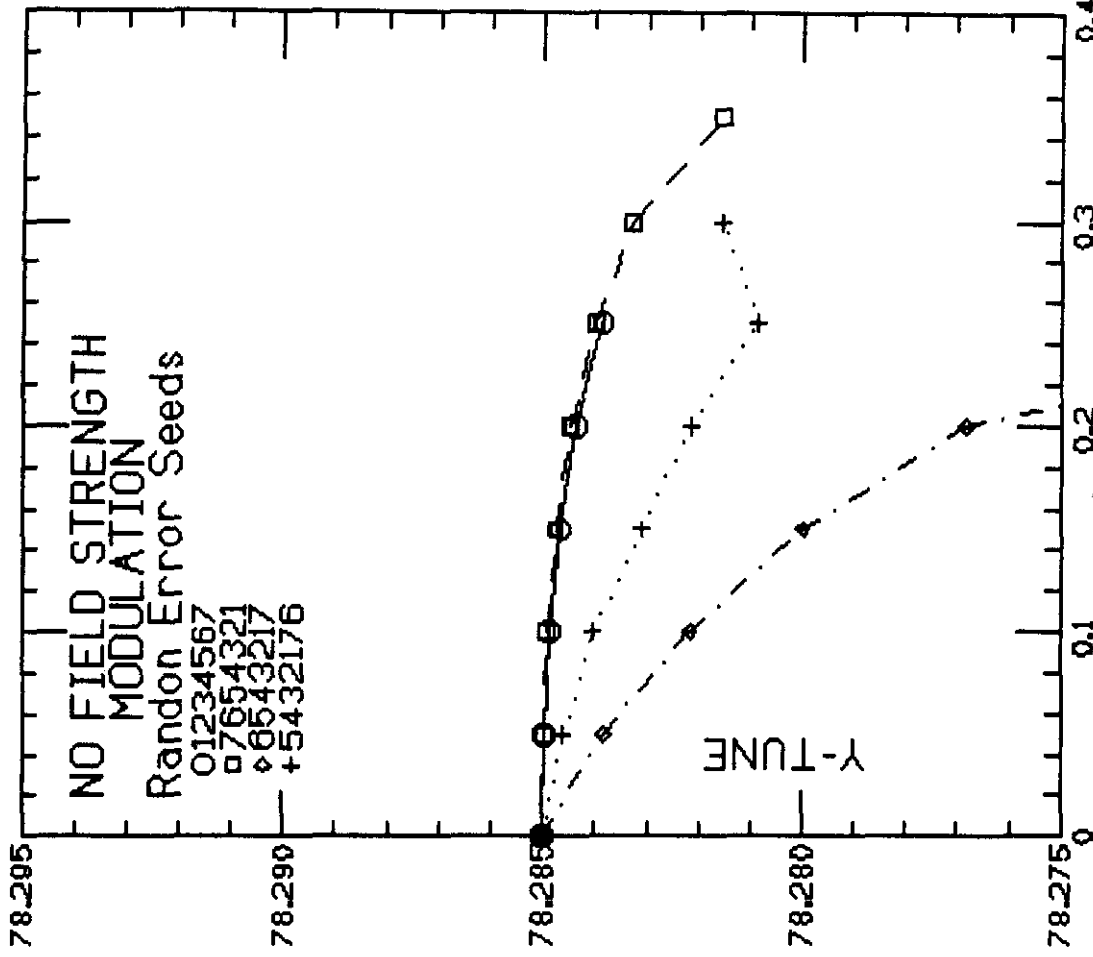
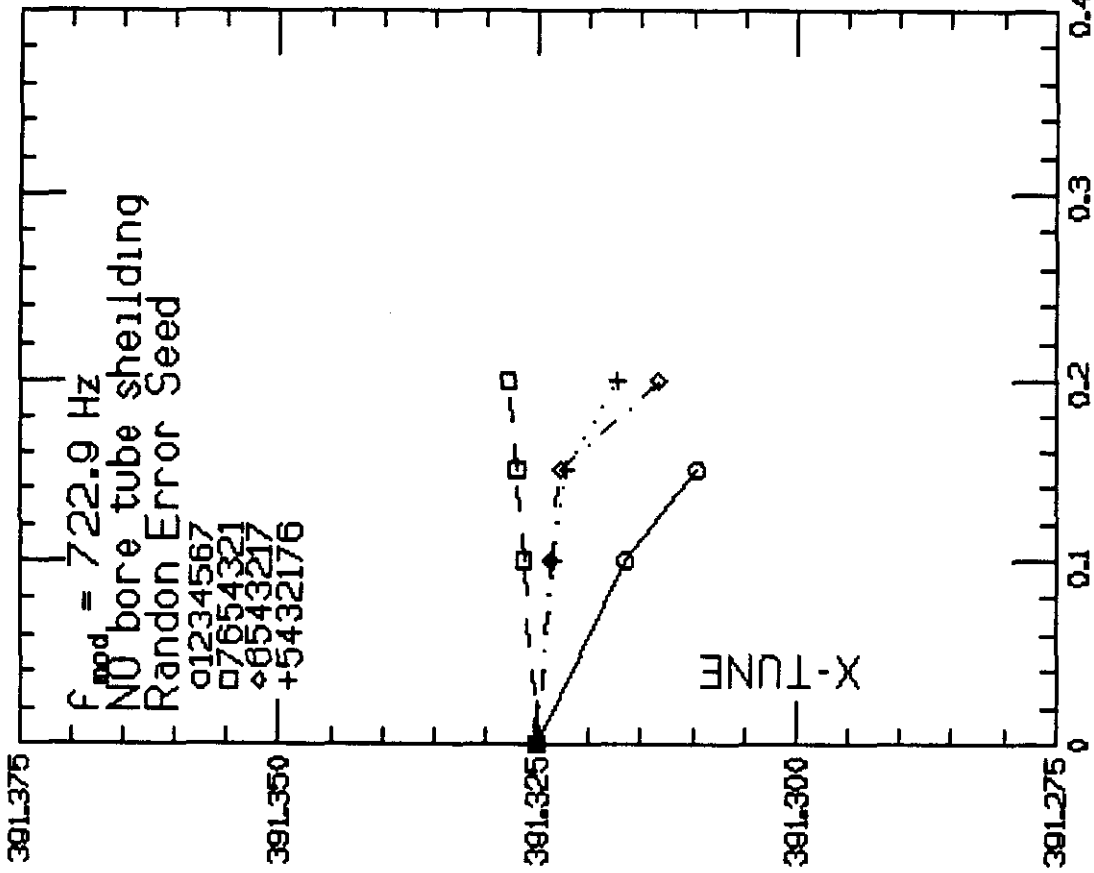
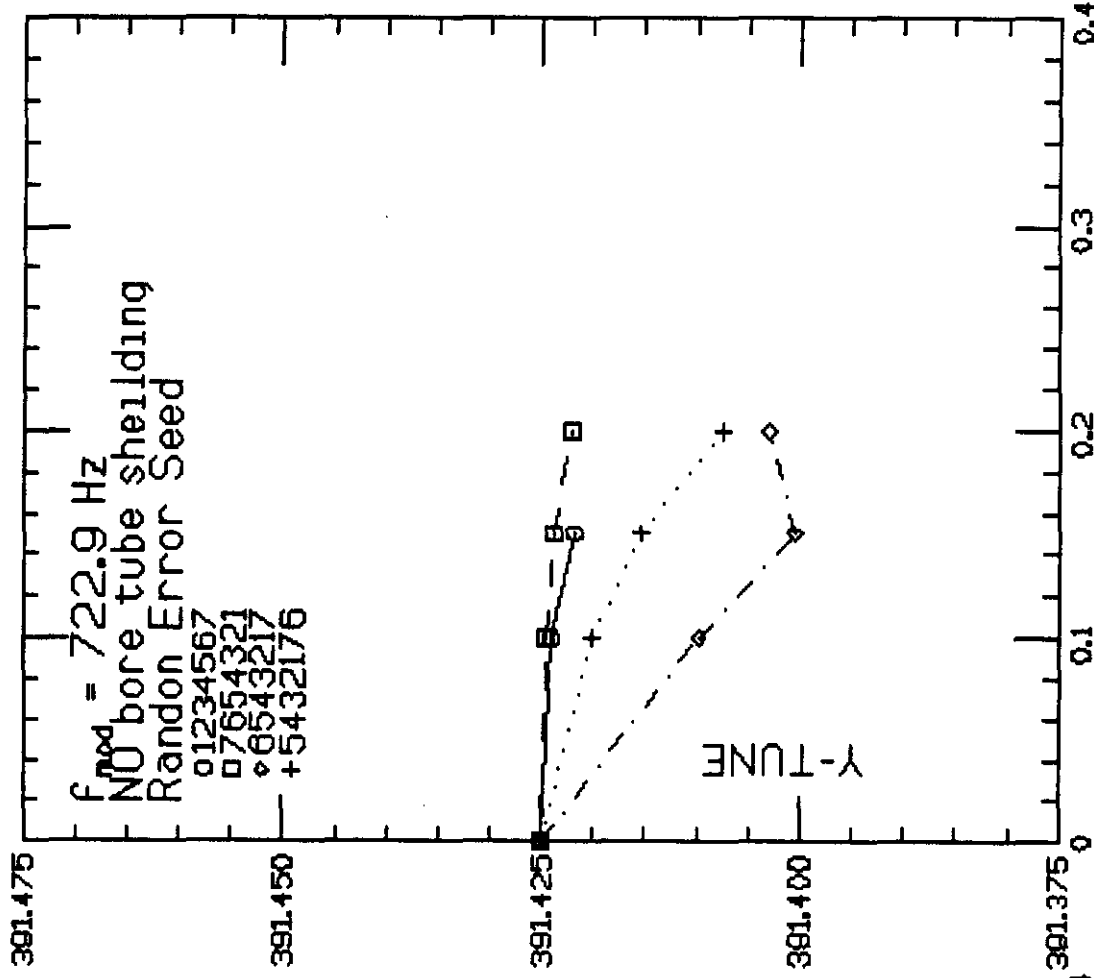


Figure 8b: The tune in the vertical direction vs launch amplitude without field strength modulation.



LAUNCH W_x (10^{-6} m)

Figure 9a: The tune (for every 5th turn) in the horizontal direction vs launch amplitude with field strength modulation (average $\Delta B/B = 10 \times 10^{-4}$).



LAUNCH W_y (10^{-6} m)

Figure 9b: The tune (for every 5th turn) in the vertical direction vs launch amplitude with field strength modulation (average $\Delta B/B = 10 \times 10^{-4}$).

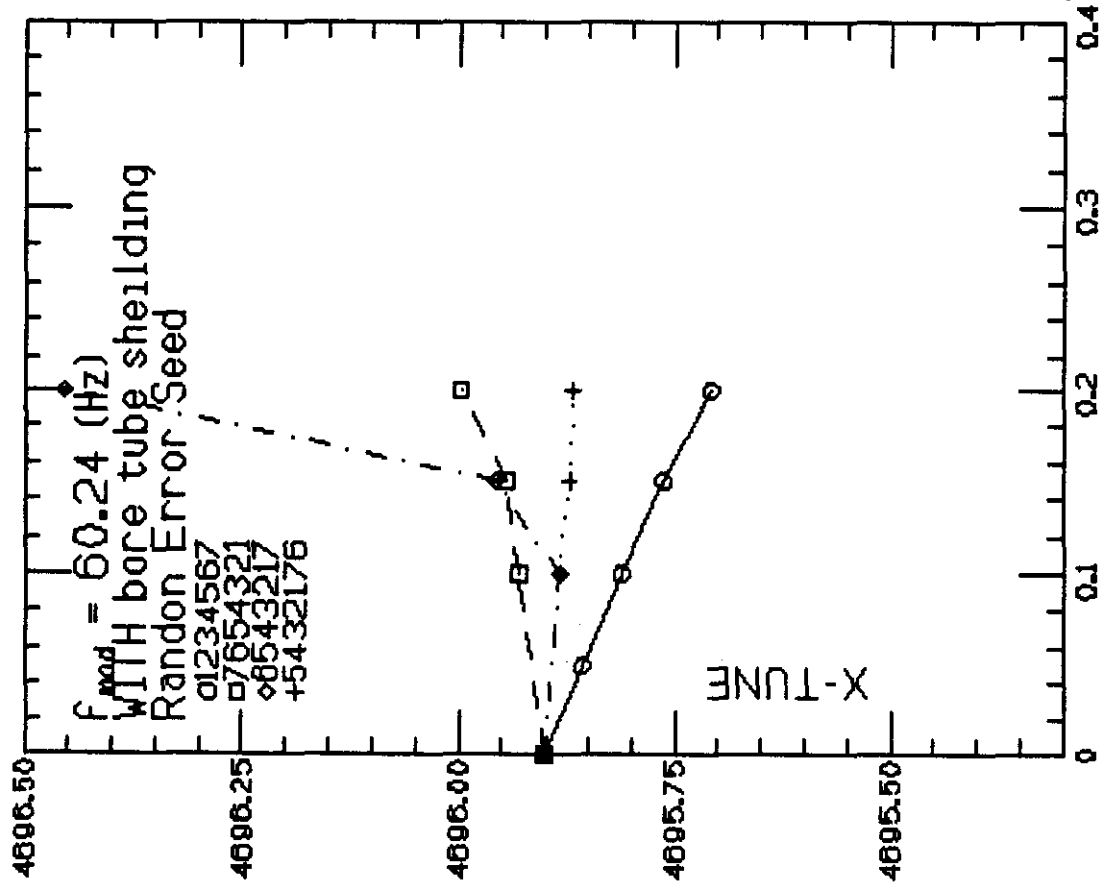


Figure 10a: The tune (for every 60th turn) in the horizontal direction vs launch amplitude with field strength modulation (average $\Delta B/B = 10 \times 10^{-4}$).

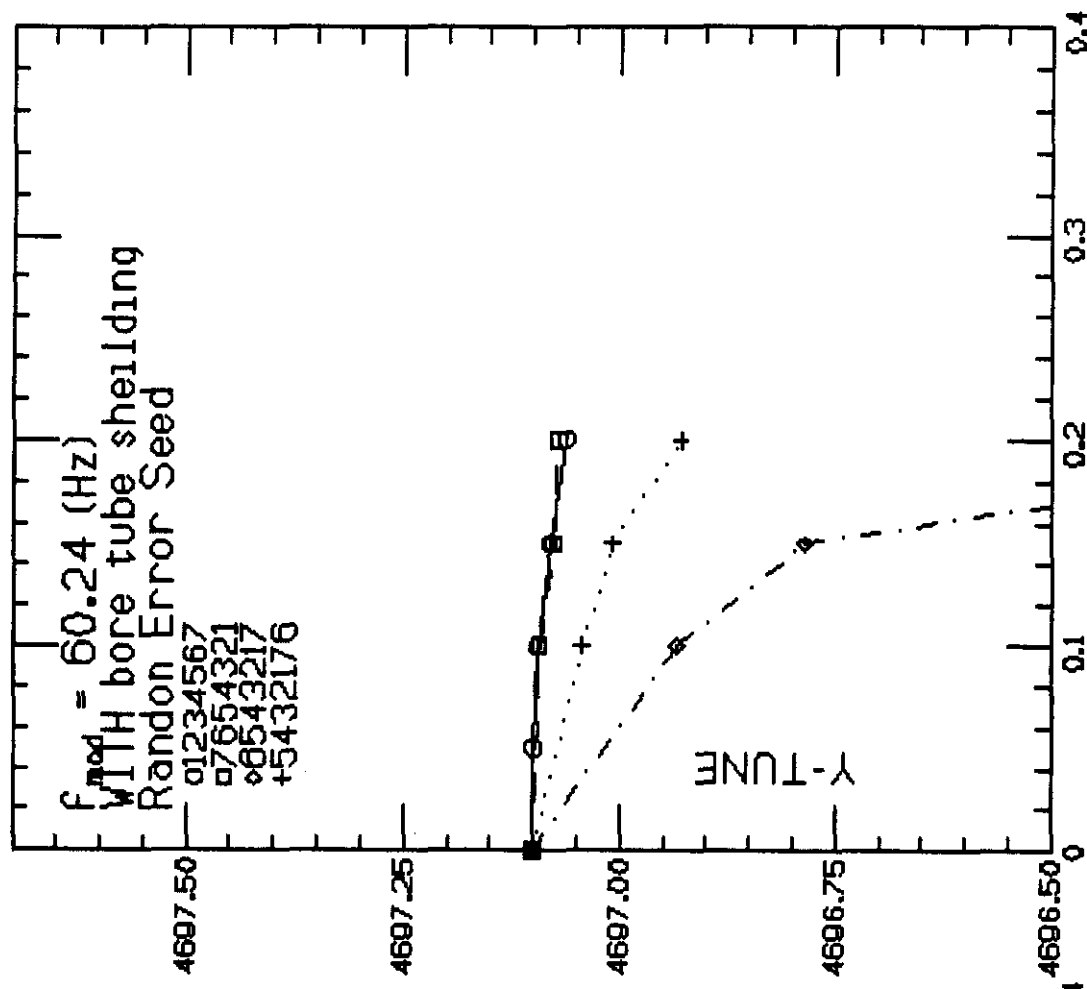


Figure 10b: The tune (for every 60th turn) in the vertical direction vs launch amplitude with field strength modulation (average $\Delta B/B = 10 \times 10^{-4}$).

References

- 1) R.E.Shafer, NAL Report TM-991, (September 22,1980)
- 2) Code developed and written by Eteine Forest (LBL) (1987)
- 3) D.A.Edwards and L.C.Teng, IEEE Trans NS-20, p.885 (1973)

